



OPEN

Influences of conservation measures on runoff and sediment yield in different intra-event-based flood regimes in the Chabagou watershed

Shan-Shan Wang^{1,2}, Zhan-Bin Li^{1✉}, Le-Tao Zhang³ & Bo Ma¹

The Loess Plateau in China has suffered severe soil erosion. To control soil erosion, extensive conservation measures aimed at redistributing rainfall, hindering flow velocity and intercepting sediment were implemented on the Loess Plateau. To accurately evaluate the combined effect of conservation measures in the Chabagou watershed, this study classified intra-event-based floods into four regimes via cluster and discriminant analyses. Regime A was characterized by short flood duration and low erosive energy, regime B was characterized by short flood duration and high erosive energy, regime C was characterized by long flood duration and low erosive energy, and regime D was characterized by long flood duration and high erosive energy. The results indicated that peak discharge (q_p), runoff depth (H), mean discharge (q_m), and runoff erosion power (E) decreased by 75.2%, 56.0%, 68.0% and 89.2%, respectively, in response to conservation measures. Moreover, area-specific sediment yield (SSY), average suspended sediment concentration (SCE), and maximum suspended sediment concentration ($MSCE$) decreased by 69.2%, 33.3% and 11.9%, respectively, due to conservation measures. The nonlinear regression analysis revealed a power function relationship between SSY and E in both the baseline (1961–1969) and measurement period (1971–1990) in all regimes. Conservation measures reduced sediment yield by not only reducing the runoff amount and soil erosion energy but also transforming the flood regime, for example, transforming a high-sediment-yield regime into a low-sediment-yield regime. Moreover, conservation measures altered the SSY - E relationship in regime A, whereas no obvious difference in regime B or C/D was observed between the measurement period and the baseline period. This study provides a better understanding of the mechanism of runoff regulation and the sediment yield reduction under comprehensive conservation measures in a small watershed on the Chinese Loess Plateau.

Soil erosion, which includes the processes of soil destruction, peeling, transport and deposition by external forces, is extremely complicated^{1–3}. Exploring the characteristics of runoff and soil erosion processes is imperative for a better understanding of the mechanisms of soil erosion. In recent decades, numerous studies have focused on the spatial and temporal heterogeneity of rainfall and other hydrological processes in watersheds^{4–8}, and the results have improved the accuracy of hydrological models in simulating the processes of rainfall and runoff generation^{9–12}. In addition, an increasing number of studies have focused on the effects of hydrological regimes on soil erosion and sediment behavior^{13,14}. Surface runoff is an erosive agent and medium for water erosion, and its flow determines the capacity for erosion and sediment transport¹⁵, parameters of which are widely used as indicators in research on sediment flow behavior^{13,15}. However, the relationships between soil erosion and hydrological processes have not been thoroughly examined, with studies and data remaining limited^{13,15}.

The Loess Plateau in China, which is highly fragmented by gullies, has suffered severe soil erosion. Since the 1970s, a series of conservation measures, including terracing, afforestation, and damming, have been

¹State Key Laboratory of Soil Erosion and Dryland Farming on the Loess Plateau, Institute of Soil and Water Conservation, Chinese Academy of Sciences and Ministry of Water Resources, Xinong Rd. 26, Yangling 712100, Shaanxi, China. ²University of Chinese Academy of Sciences, Beijing 100049, China. ³College of Environment and Planning, Henan University, Kaifeng 475004, Henan, China. ✉email: zhanbinli@126.com

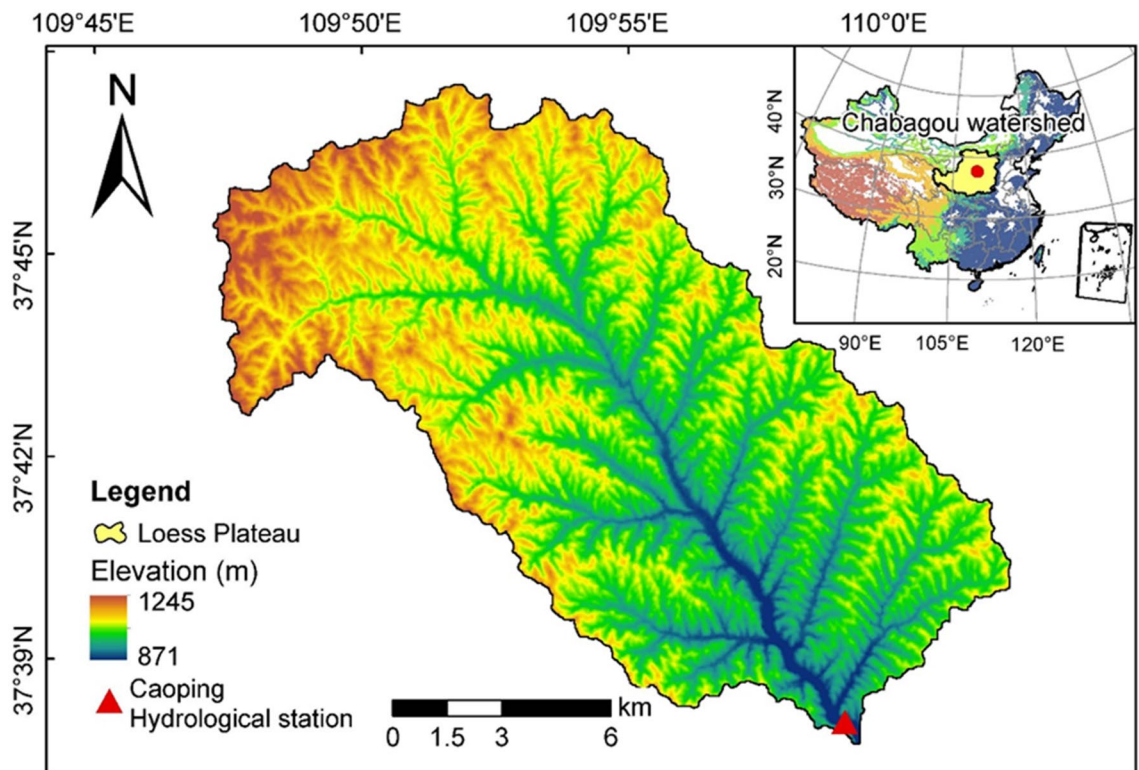


Figure 1. Map of the Chabagou watershed. The map was generated with ESRI ArcMap 10.5 software (<http://www.esri.com/arcgis/>) with terrain data acquired from the Advanced Land Observing Satellite (ALOS) Phased Array type L-band SAR (PALSAR) Radiometric Terrain Corrected high-resolution dataset⁴².

implemented on the Loess Plateau to prevent soil and water loss and maintain agricultural productivity^{16,17}. By applying the WATEM/SEDEM erosion model, Boix-Fayos et al.¹⁸ found that changes in land use in the absence of check dams decreased the sediment yield by 54%, whereas with check dams but without land use changes, 77% of the sediment yield was retained. Terraces, a type of conservation measure, can favor water infiltration, soften steep mountainous slopes and reduce runoff and soil erosion¹⁹. Mulching also has profound influences on infiltration, surface runoff, soil moisture and erosion; mulch cover of 2 t/ha and 4 t/ha has been found to reduce the runoff peak by 21% and 51%, respectively²⁰. Conservation measures can not only reduce soil erosion but also modify flow regimes^{21–23}. However, research is lacking on the effect of conservation measures on the relationship between runoff and sediment in different surface runoff regimes. Given the complexity of conservation measures on the Loess Plateau, it is difficult to isolate the influences of individual measures on stream flow²³. Therefore, it may be beneficial to investigate the combined effects of conservation measures on the sediment flow of the watershed and the runoff-sediment relationship by analyzing data from a watershed outlet station.

The aims of this study were to (1) assess the integrated effects of conservation measures on surface runoff and sediment in the Chabagou watershed, (2) classify intra-event-based floods and explore the influence of conservation measures on the intra-event-based flood regime, and (3) evaluate the changes in the runoff-sediment relationship due to conservation measures in different flood regimes. This study is expected to provide a better understanding of the mechanism of sediment reduction due to conservation measures at the watershed scale.

Study area, data source and treatments

Study area. The Chabagou watershed has nested hydrological stations, long time series of measured hydrological and sediment data and complete meteorological data, which are important in geomorphic process research, hydrological simulation and sediment research in the hilly and gully region of the Loess Plateau. The Chabagou watershed (109°47' E, 37°31' N), which is part of the first region of the gullied and rolling Loess Plateau, is a first-order tributary region of the Dali River. The Chabagou watershed, with an area of 205 km² and a channel length of 26.5 km, is symmetric in shape, and its elevation ranges from 900 to 1100 m. Its average annual precipitation is approximately 450 mm. The rainfall distribution is uneven throughout the year, with 70% of the total rainfall being concentrated from June to September, mostly as strong intensity and short-duration rainstorms. The temperature varies from – 27 to 38 °C, and the annual average temperature is 8 °C. Due to loose soil, sparse vegetation, heavy rainfall intensity, etc., the region suffers severe soil erosion. The average annual erosion modulus is 22,200 t km⁻², and the maximum and minimum annual erosion moduli are 71,100 t km⁻² and 2110 t km⁻², respectively. The Caoping hydrological station (Fig. 1), which services a catchment area of 187 km², a channel length of 24.1 km and an average gully channel gradient of 7.57‰, is set at the watershed outlet to observe the hydrology and sediment conditions.

During the 1961–1969 observation period, the Chabagou watershed was in a near-natural state, with little artificial disturbance²⁴. A series of conservation measures were initiated in the Chabagou watershed in 1970. By 1990, there were 21.13 km² of terraced fields, 8.63 km² of afforestation, 2.13 km² of planted grass and 4.07 km² of dammed land in the Chabagou watershed. The total treatment area was 35.96 km², which accounted for 17.54% of the watershed. Based on the double-accumulative curve method and considering that engineering measures such as dams and terraces reached their peak in the 1970s, Qi Junyu concluded that soil and water conservation measures were effective in 1970²⁵. Hence, 1961–1969 and 1971–1990 were regarded as the baseline period and measurement period, respectively²⁵.

Data source and treatments. The hydrological and sediment data are from a hydrological experiment at the Zizhou runoff experimental station, which was set up by the Yellow River Water Conservancy Committee (1961–1990, excluding 1970) (Loess Plateau Data Center, National Earth System Science Data Sharing Infrastructure, National Science & Technology Infrastructure of China (<http://loess.geodata.cn>)). The collection of all the water and sediment data, including water level, flow rate, sediment concentration and sediment yield, as well as sampling and experimental analysis, was performed in strict accordance with national standards²⁶.

According to relevant test standards of the hydrological station²⁷, a flood runoff event with a runoff depth ≥ 0.1 mm, a peak flow rate ≥ 1 m³/s, and a duration ≥ 450 min was defined as a main channel flood event (at Caoping hydrological station). A total of 49 flood events from 1961 to 1969 and 82 flood events from 1971 to 1990 were selected.

Indicators such as flood duration (T , min), time-to-peak (T_p , min), duration of recession (T_r , min), peak discharge (q_p , m³ s⁻¹), runoff depth (H , mm), mean discharge (q_m , m³ s⁻¹), flow variability (FV), and runoff erosion power (E , m⁴ s⁻¹) were selected to reflect the runoff characteristics of intra-event-based floods. E is the product of the peak discharge and runoff depth, and it represents the average efficiency of the combined effects of natural rainfall characteristics and the underlying surface characteristics of the basin on erosion and sediment yield in the basin²⁸.

The sediment characteristics of intra-event-based floods were reflected by indicators such as area-specific sediment yield (SSY , t km⁻²), average suspended sediment concentration (SCE , kg m⁻³), maximum suspended sediment concentration ($MSCE$, kg m⁻³) and sediment variability (SCV). The calculation formulas of these indicators were as follows:

$$\text{Mean runoff depth : } H = \frac{\sum q \Delta t}{A}$$

$$\text{Mean discharge : } q_m = \frac{\sum q \Delta t}{T}$$

$$\text{Flow variability : } FV = \frac{q_p}{q_m}$$

$$\text{Runoff erosion power : } E = q_p H$$

$$\text{Sediment yield : } ESY = \sum S q \Delta t$$

$$\text{Area - specific sediment yield : } SSY = \frac{ESY}{A}$$

$$\text{Average suspended sediment concentration : } SCE = \frac{SSY}{H}$$

$$\text{Sediment variability : } SCV = \frac{SCE}{MSCE}$$

where Δt represents the time interval of hydrological observation (min); q_p , q_m , H , FV and E represent the peak discharge (m³ s⁻¹), mean discharge (m³ s⁻¹), runoff depth (mm), flow variability and runoff erosion power (m⁴ s⁻¹), respectively; and S , SCE , $MSCE$, ESY , SSY and SCV represent the instantaneous sediment concentration (kg m⁻³), average suspended sediment concentration (kg m⁻³), maximum suspended sediment concentration (kg m⁻³), sediment yield (t), area-specific sediment yield (t km⁻²) and sediment variability, respectively.

Study method. Based on the flood runoff characteristics, intra-event-based flood events in 1961–1969 were classified into different flood process regimes using cluster analysis and discriminant analysis^{29,30}. Zhang^{13,31} and other researchers^{32,33} performed similar research on the classification of flood events using cluster analysis, and they adopted flood duration, runoff depth and peak discharge as indices. Runoff depth can reflect the precipitation amount and the influence of the underlying surface of a watershed on the rainfall redistribution, and peak discharge can reflect the temporal and spatial distributions of rainfall and the effect of the underlying surface of the watershed on the confluence process²⁸. Flood duration is one of the main indices of rainfall type³⁴. Thus, we adopted the following variables as classification indices: flood duration (T), runoff depth (H) and peak discharge

Statistic	T	T_p	T_r	q_p	H	q_m	FV	E	SSY	SCE	$MSCE$	SCV
1961–1969												
Minimum	465	3	399	1.19	0.14	0.50	2.2	0.0002	12.1	58.0	98.5	1.1
Maximum	3360	1182	2865	1520	36.26	48.08	46.5	43.1	28,143.8	976.4	1220.0	2.3
Mean	1540.1	230.0	1310.0	209.51	4.97	11.09	17.7	2.7	3640.0	649.6	825.1	1.3
Std. deviation	703.4	266.8	617.9	290.4	6.6	12.5	9.8	8.0	5196.7	188.6	192.8	0.3
CV	0.5	1.2	0.5	1.4	1.3	1.1	0.6	3.0	1.4	0.3	0.2	0.2
1971–1990												
Minimum	492	4	366	2.35	0.18	0.37	2.1	0.0005	11.2	54.6	107.0	1.1
Maximum	3810	576	3714	447	15.51	21.47	47.6	5.0	9898.1	808.6	1030.0	4.6
Mean	1794.9	102.3	1692.6	51.97	2.16	3.60	13.2	0.3	1121.8	438.1	726.5	1.8
Std. deviation	739.3	107.8	733.5	72.5	2.7	4.0	7.9	0.7	1611.1	176.6	202.4	0.7
CV	0.4	1.1	0.4	1.4	1.2	1.1	0.6	2.7	1.4	0.4	0.3	0.4

Table 1. Descriptive statistics of the characteristics of event-based flood flows and sediment in 1961–1990 (excluding 1970). There were 49 and 82 recorded events in 1961–1969 and 1971–1990, respectively, included in the statistical analyses. CV coefficient of variation; T flood event duration, in min; T_p time-to-peak, in min; T_r duration of recession, in min; q_p peak discharge, in $m^3 s^{-1}$; H runoff depth, in mm; q_m mean discharge, in $m^3 s^{-1}$; FV flow variability, which is defined as the ratio of the event-based flood peak discharge to mean discharge; E runoff erosion power, in $m^4 s^{-1}$; SSY area-specific sediment yield, in $t km^{-2}$; SCE average suspended sediment concentration, in $kg m^{-3}$; $MSCE$ maximum suspended sediment concentration, in $kg m^{-3}$; SCV sediment variability, which is defined as the ratio of the maximum to average suspended sediment concentration at the event timescale. The same note also applies to Table 2.

(q_p). After repeated trial and error tests, hierarchical cluster analysis and discriminant analysis were selected to classify the flood events at the Caoping hydrological station in 1961–1969.

The basic idea of a hierarchical cluster analysis is to first cluster variables with similar distances according to distance and then sequentially cluster variables with more distant distances until each variable is placed into a suitable cluster. The process of hierarchical cluster analysis in SPSS is as follows: Assuming that there are n variables in a data set, the first step is to determine the basic meaning of the distance and the calculation method of the distance between classes. In the second step, these n variables are grouped into a class, and there are n classes in total. In the third step, variables with similar distances are grouped into one class according to the calculated interclass distance, and other variables are still classified into one class. In this case, there are $n-1$ classes. The fourth step is to further aggregate the classes that are near each other, yielding $n-2$ classes. The process continues sequentially until all of the data are fully grouped into a category. The Ward method and Euclidean distance were used in the hierarchical cluster analysis, and the Fisher discriminant function was used in the discriminant analysis. Based on this classification, the intra-event-based flood events in 1971–1990 were discriminated.

Cluster analysis, discriminant analysis, regression analysis and other data analysis processes were performed using SPSS 18.0. Origin 12.5 was used to prepare figures.

Results

Effects on intra-event-based flood runoff and sediment characteristics. Between the 1960s and 1990s, there was no significant change in rainfall in the Chabagou watershed³⁵. The mean values of runoff and sediment transport in the baseline period and measurement period were calculated. Regardless of rainfall influence, the effect of conservation measures was assessed by the time series contrasting method²⁵.

Table 1 shows the statistics of the characteristics of event-based flood flows and sediment in 1961–1990 (excluding 1970). Compared with those in the baseline period, T and T_r in the measurement period increased by 16.54% and 29.21%, respectively; however, T_p decreased by 55.52% in the measurement period, which showed that the soil and water conservation measures extended the flood duration while reducing the time of increased discharge. Under identical rainfall conditions, long-duration runoff with less time for increased discharge could cause less erosion than short-duration runoff with more time for increased discharge³⁶. Hence, the conservation measures reduced soil erosion by prolonging the flood duration and reducing the time to peak. In addition, the hydrodynamic indices q_p , H and q_m were 75.2%, 56.0% and 68.0% lower, respectively, in the measurement period than in the baseline period. Moreover, E in the measurement period was only 10.2% that in the baseline period. The results showed that the conservation measures greatly reduced the hydrodynamic energy and thus soil erosion. In addition, the relative erosion indicators SSY , SCE and $MSCE$, decreased 69.2%, 33.3%, and 11.9%, respectively, in the measurement period compared with the baseline period, which indicated that the conservation measures significantly reduced soil erosion and decreased the mean sediment concentration, although the reduction in the maximum sediment concentration was relatively small. The conservation measures, especially the engineering measures, reduced the runoff velocity, extended the flood duration, and reduced the peak discharge, which sharply reduced the runoff erosion power^{37,38}. As a consequence of the decrease in erosive energy, soil erosion was diminished.

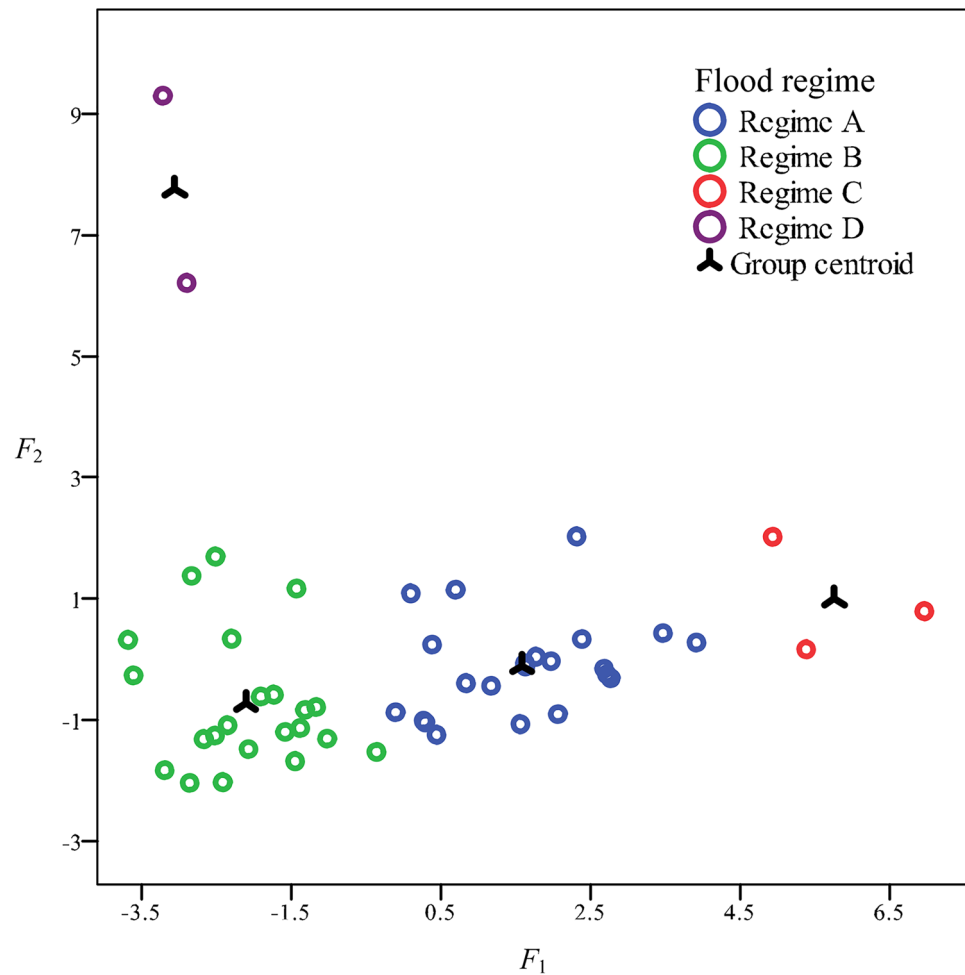


Figure 2. Discriminant analysis of different flood regimes in 1961–1969. F_1 and F_2 represent the scores of discriminant functions. Regime A: short flood duration and low erosive energy; Regime B: short flood duration and high erosive energy; Regime C: long flood duration and low erosive energy; Regime D: long flood duration and high erosive energy.

Influence on intra-event-based flood regimes. *Classification of flood events and the characteristics of baseline period flood regimes.* Figure 2 shows the clustering results of the flood events at the Caoping hydrological station in 1961–1969. The flood events were divided into 4 regimes with a significance level of $p < 0.001$. The data in the scatter diagrams of different discriminant functions were clustered, which indicated that the classification results were reasonable.

The discriminant functions were as follows:

$$F_1 = 0.004T + 0.001q_p - 0.22H - 4.6$$

$$F_2 = 0.001T - 0.001q_p + 0.292H - 2.581$$

$$F_3 = 0.008q_p - 0.305H - 0.76$$

The classification functions of the different regimes were as follows:

$$D_1 = 0.025T + 0.01q_p - 0.878H - 23.927$$

$$D_2 = 0.011T + 0.007q_p - 0.24H - 6.495$$

$$D_3 = 0.04T + 0.013q_p - 1.456H - 61.74$$

$$D_4 = 0.014T + 2.445H - 56.302$$

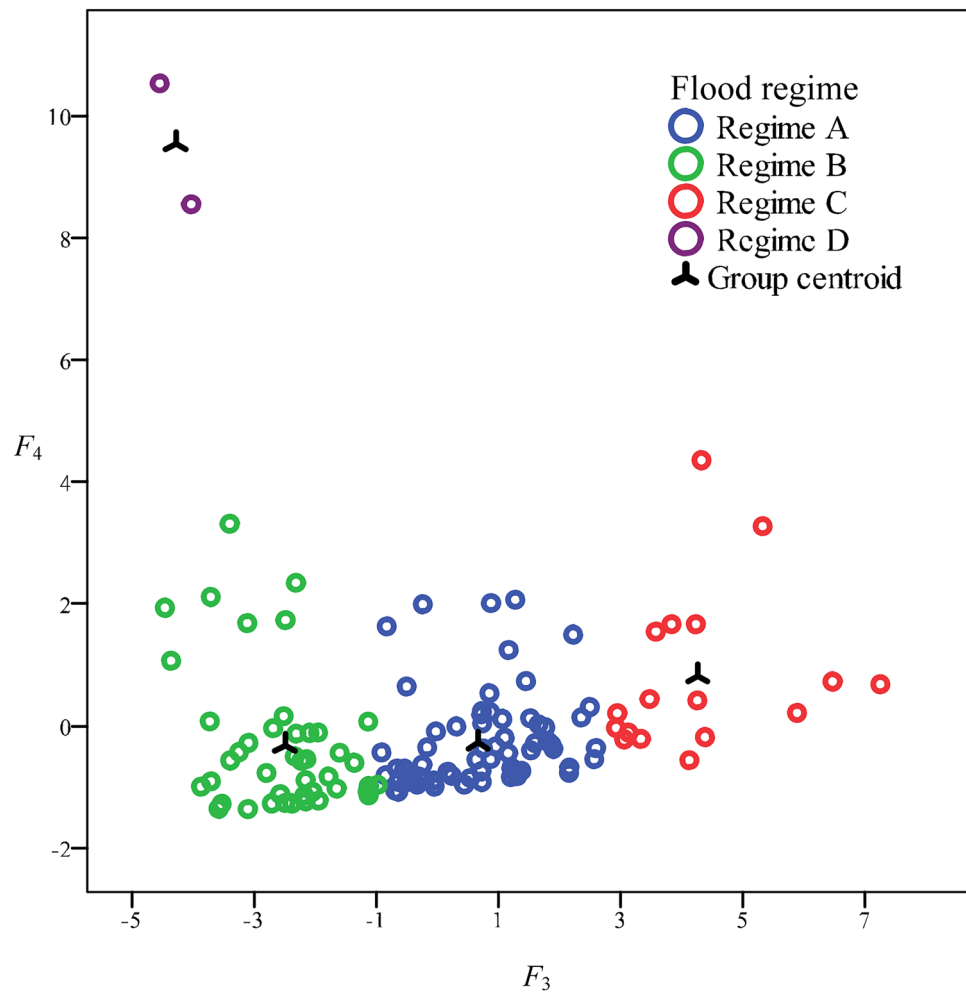


Figure 3. Discriminant analysis of different flood regimes in 1961–1990 (excluding 1971). F_3 and F_4 represent the scores of discriminant functions. Regime A: short flood duration and low erosive energy; Regime B: short flood duration and high erosive energy; Regime C: long flood duration and low erosive energy; Regime D: long flood duration and high erosive energy.

where F_1 , F_2 , and F_3 represent the scores of discriminant functions and D_1 , D_2 , D_3 and D_4 represent the classification scores of regimes A, B, C and D, respectively.

Based on the classification of the baseline period (1961–1969), the flood events of the measurement period (1971–1990) were discriminated with a significance level of $p < 0.001$; Fig. 3 presents the cluster results. The classification results were reasonable considering the scatter diagrams of the different discriminant functions.

The discriminant functions were as follows:

$$F_4 = 0.003T + 0.001q_p - 0.233H - 5.2$$

$$F_5 = 0.001q_p + 0.288H - 1.621$$

$$F_6 = 0.011q_p - 0.447H - 0.65$$

The classification functions of the different regimes were as follows

$$D_5 = 0.021T + 0.014q_p - 1.279H - 19.749$$

$$D_6 = 0.01T + 0.011q_p - 0.54H - 6.1$$

$$D_7 = 0.034T + 0.018q_p - 1.779H - 49.331$$

$$D_8 = 0.007T + 0.018q_p + 2.695H - 64.322$$

Year	Regime/N	T	T _p	T _r	q _p	H	q _m	FV	E	SSY	SCE	MSCE	SCV	PR
1959–1969	A/21	1878.81	293.48	1585.33	129.00	3.40	5.52	21.50	0.68	2388.62	643.74	823.29	1.33	42.86
	B/22	906.59	129.18	777.41	215.20	4.26	14.41	12.39	1.72	3229.82	661.17	810.25	1.27	44.90
	C/4	2963.25	423.75	2539.50	77.45	3.43	3.60	23.30	0.33	1731.95	553.70	848.00	1.58	8.16
	D/2	2105.50	286.00	1819.50	1256.50	32.33	47.88	26.22	39.58	25,108.29	776.84	961.00	1.24	4.08
1971–1990	A/47	1822.68	100.23	1722.45	38.42	1.69	2.66	12.77	0.14	801.30	414.27	740.87	1.97	57.32
	B/22	994.91	93.64	901.27	49.04	1.64	5.02	9.15	0.22	907.39	446.32	655.86	1.62	26.83
	C/13	3048.31	124.46	2923.85	105.92	4.78	4.56	21.43	0.87	2643.32	510.20	793.92	1.78	15.85

Table 2. Descriptive statistics of the characteristics of event-based flood flows and sediment under different flood regimes in 1961–1990 (excluding 1970). Regime A: short flood duration and low erosive energy; Regime B: short flood duration and high erosive energy; Regime C: long flood duration and low erosive energy; Regime D: long flood duration and high erosive energy. *N*, the number of recorded flood events in the regime; PR, the proportion of the number of recorded flood regimes to the total flood number at different times, in %. Other indicators are as defined in Table 1.

where F_4 , F_5 , and F_6 represent the scores of discriminant functions and D_5 , D_6 , D_7 and D_8 represent the classification scores of regimes A, B, C and D, respectively.

Table 2 describes the classification results and the characteristics of different flood regimes. During the baseline period, the flood durations of regimes A and B were short, whereas the flood durations of regimes C and D were long. The q_p , H , E , SSY and SCE of regime A, which accounted for 42.86% of all flood events, were small. The T of regime B, which accounted for 44.90% of the flood events, was the shortest, but the q_p , H , E , SSY and SCE of regime B were large. Regime C, which accounted for 8.16% of all flood events, had the longest T , but the q_p , H , E , SSY and SCE of regime C were small. The q_p , H , E , SSY and SCE of regime D, which represented 4.08% of all flood events, were the largest. The runoff erosive energies of regimes A and C were smaller than those of regimes B and D, respectively.

Effect on intra-event-based flood regimes. The average T of the measurement period was 1.17 times longer than the T of the baseline period. In addition, q_p decreased by 75.2% in the measurement period. E in the measurement period accounted for only 10.2% of that in the baseline period (Table 1). Consequently, in the measurement period, the flood events transitioned from regimes B and D, which have high erosive energy, to regimes A and C, which have low erosive energy. Compared with those in the baseline period, the proportions of regime A and regime C flood events increased by 33.7% and 94.2%, respectively, during the measurement period; regime B flood events decreased from 44.9% to 26.8%, and regime D flood events did not occur in the measurement period.

Because the conservation measures weakened the erosive energy of runoff, other characteristics within the same regime changed between the measurement period and baseline period. The q_p , H , SSY and SCE of regimes A and B were smaller in the measurement period than in the baseline period, and the E of regimes A and B decreased by 79.6% and 87.4%, respectively, in the measurement period. Due to the increase in T and the decrease in erosion in the measurement period, regime D, which is the regime with the maximum erosive ability, transitioned into regime C, which has a long T and low erosive energy. Therefore, the variables of regime C, such as T , q_p , H , q_m , SSY and SCE , increased in the measurement period compared with the baseline period. In addition, the q_p , H , q_m , SSY and SCE of regime C were larger than those of regimes A and B in the measurement period and smaller than those of regime D and regimes C/D in the baseline period.

Discussion

Effect on sediment yield. Comparisons of the runoff and sediment characteristics between the baseline period (1961–1969) and measurement period (1971–1990) showed that SSY , SCE and $MSCE$ decreased by 69.2%, 33.3% and 11.9%, respectively, in the measurement period. The extensive implementation of afforestation, grass planting and terracing measures and, especially, the large-scale construction of check dams^{16,39,40} has profoundly affected the physical characteristics of the underlying surface, the erosional environment and the surface hydrological processes of the watershed, thus changing the total amount and temporal distribution of flood runoff. Accordingly, these measures have resulted in the redistribution of runoff erosion energy and changed the dynamic processes to control soil and water loss.

The conservation measures delayed runoff formation, increased soil infiltration and intercepted rain^{20,41}, thereby causing q_p , H and q_m to decrease by 75.2%, 56.0% and 68.0%, respectively. Hence, the runoff erosion energy was reduced; for example, E in the measurement period was only 10.2% of that in the baseline period.

After repeated trial and error, selection of the T , q_p , H indicators and cluster and discriminant analyses, the flood events in the baseline period (1961–1969) at the Caoping hydrological station were classified into four regimes, and the runoff and sediment characteristics in the different regimes were investigated. The flood durations of regimes A and B were shorter, whereas those of regimes C and D were longer. In addition, regimes A and C produced less sediment yield and lower soil erosion energy; in contrast, regimes B and D produced more sediment yield and higher soil erosion energy. This research illustrated that different sediment characteristics occurred in different flood regimes. Therefore, the conservation measures achieved the purpose of reducing

sediment yield by not only reducing runoff amount or soil erosion energy but also transforming flood regimes, for example, transforming a high-sediment-yield regime into low-sediment-yield regime.

Effect on intra-event-based flood regimes. The conservation measures prolonged the flood duration, decreased the peak discharge and runoff depth, and transformed the high-sediment-yield regimes B and D into the low-sediment-yield regimes A and C; notably, regime D, which had the most sediment yield, did not occur in the measurement period. Because regime D did not occur in this period and because the conservation measures transformed regime D into regime C, regimes C and D in the baseline period were merged. By nonlinear fitting of SSY and E in the baseline and measurement periods, a power function relationship between SSY and E , with all $R^2 > 0.8$, was discovered. The SSY - E regression lines were compared between the baseline and measurement periods in different regimes. The SSY and E relationship in regime A obviously changed in the measurement period; however, there was no obvious change in regime B or C/D. This result indicated that conservation measures could change the runoff and sediment relationship in regimes with low sediment yields. However, because the relationship between runoff and sediment remains approximately constant and because the “self-regulation” of flood runoff shows limited potential for sediment reduction²⁴, the conservation measures in regimes with high sediment yields could reduce sediment yield only by reducing the runoff amount or soil erosion energy. Moreover, the conservation measures weakened the runoff erosion energy; for example, the concentration range of E (75% of the number of flood events) in the measurement period was less than that of the baseline period in all regimes.

Mechanism analysis based on runoff erosion power. H and q_p are two important parameters that reflect intra-event flood characteristics. H represents the total amount of runoff generated by heavy rain in the basin, which indirectly reflects the precipitation amount and the influence of the underlying surface of the watershed on the redistribution of rainfall. q_p represents the flood intensity, which indirectly reflects the temporal and spatial distribution of rainfall and the effect of the underlying surface of the watershed on the confluence process. Therefore, E , which is the product of runoff depth and flood peak flow²⁸, was chosen to represent erosion energy to explore the relationship between area-specific sediment yield (SSY) and E under different regimes in the baseline period (1961–1969) and the measurement period (1971–1990).

Because conservation measures prolong flood duration and reduce runoff erosion energy, regime D transitioned to regime C in the measurement period. In addition, given that the number of events in regimes C and D in the baseline period was low, regimes C and D in the baseline period were combined for the regression analysis of the SSY - H relationship. As shown in Fig. 4, the regression line for the baseline period, during which no large-scale conservation measures were carried out, plotted higher than that for the measurement period, indicating that the conservation measures generally reduced sediment yield in the watershed. Additionally, in regime A, the E of 75% of the flood events in the baseline period ranged from 0.095 to 4.501 $m^4 s^{-1}$, whereas that in the measurement period was in the range of 0.001–0.062 $m^4 s^{-1}$. In addition, the regression lines were obviously different between the baseline and measurement periods. The SSY of the measurement period was less than that of the baseline period with the same E , although the difference gradually decreased as E increased. In other words, the conservation measures not only reduced the runoff erosion energy but also changed the relationship between SSY and E . In the plots for regimes B and C/D, the regression lines of the baseline and measurement periods were almost coincident; however, those of the measurement period plotted slightly lower than those of the baseline period, indicating that in regimes B and C/D, the reductions in soil and water loss were not driven by changes in the relationship of SSY and E . In the baseline period, the E values of most flood events (75%) were 0.149–10.765 $m^4 s^{-1}$ and 0.341–43.153 $m^4 s^{-1}$ in regime B and regime C/D, respectively. However, in the measurement period, the E of most flood events (75%) varied from 0.001 to 0.101 $m^4 s^{-1}$ in regime B and varied from 0.001 to 0.347 $m^4 s^{-1}$ in regime C. Hence, the conservation measures reduced the sediment yield mainly by reducing the runoff erosion energy.

Conclusion

In total, 49 flood events from 1961 to 1969 (baseline period) and 82 flood events from 1971 to 1990 (measurement period) were selected for assessment. Compared with those in the baseline period, the runoff characteristics (q_p , H , q_m and E) and sediment characteristics (SSY , SCE and $MSCE$) of floods in all regimes benefited from the conservation measures in the measurement period.

Based on hierarchical cluster analysis and discriminant analysis, the flood events of the Caoping hydrological station were classified into four regimes: regime A, with short flood duration and low erosive energy; regime B, with short flood duration and high erosive energy; regime C, with long flood duration and low erosive energy; and regime D, with long flood duration and high erosive energy.

The conservation measures transformed the high-sediment-yield B and D regimes to the low-sediment-yield A and C regimes and changed the relationship between SSY and E in regime A. The conservation measures had little effect on the SSY - E relationship in the high-sediment-yield B and C/D regimes. Additionally, E was lower in the measurement period than in the baseline period in all regimes. This study provides evidence of the mechanism of runoff regulation and the sediment yield reduction benefit of conservation measures.

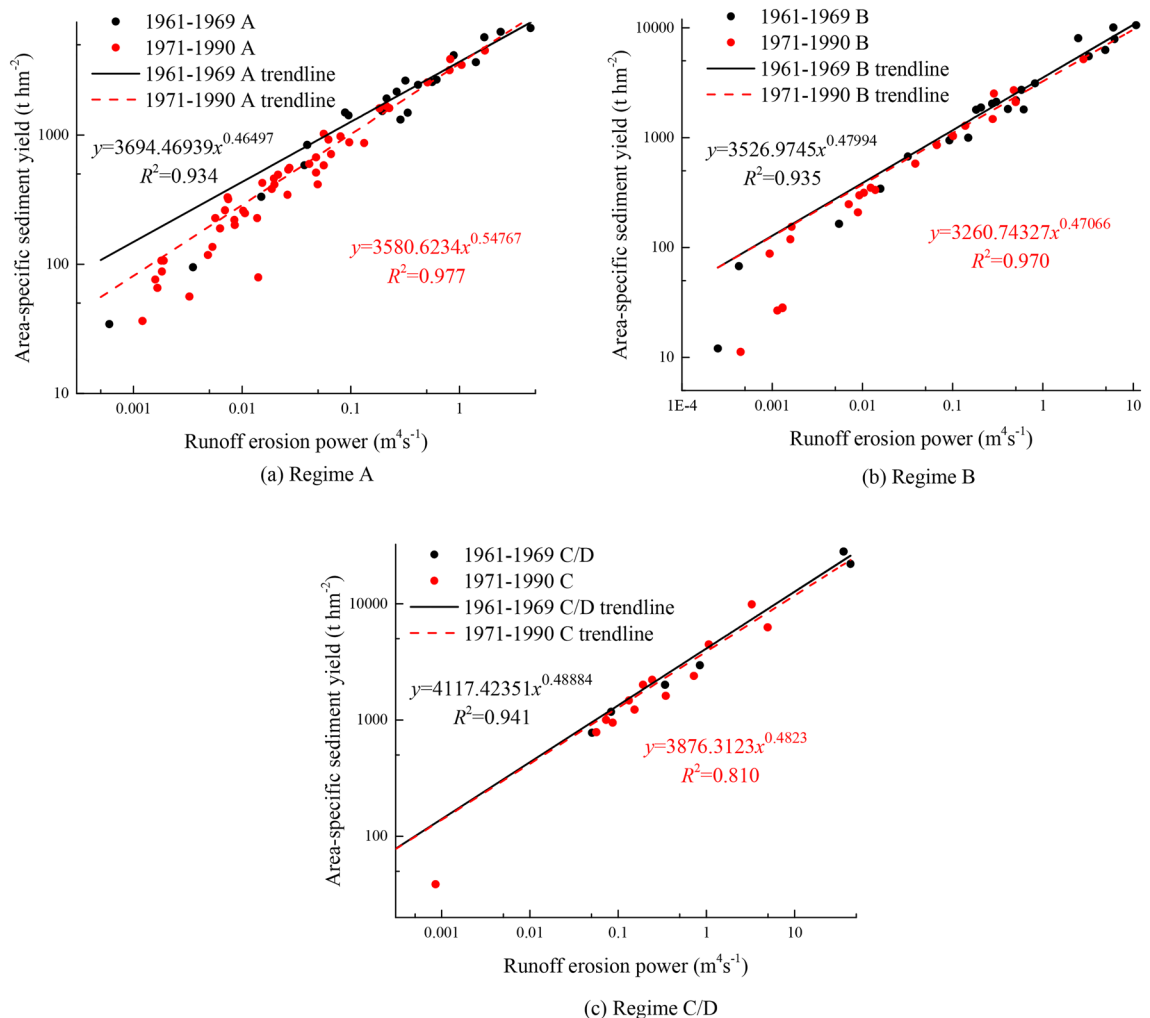


Figure 4. Correlation of area-specific sediment yield and runoff erosion power of different event-based flood regimes at different times. Regime A: short flood duration and low erosive energy; Regime B: short flood duration and high erosive energy; Regime C: long flood duration and low erosive energy; Regime D: long flood duration and high erosive energy.

Received: 8 April 2021; Accepted: 21 July 2021
Published online: 02 August 2021

References

1. Mayor, A. G., Bautista, S. & Bellot, J. Scale-dependent variation in runoff and sediment yield in a semiarid Mediterranean catchment. *J. Hydrol.* **397**, 128–135 (2011).
2. Zoccatelli, D., Borga, M., Zanon, F., Antonescu, B. & Stancalie, G. Which rainfall spatial information for flash flood response modelling? A numerical investigation based on data from the Carpathian range, Romania. *J. Hydrol.* **394**, 148–161 (2010).
3. Lopezarazon, J. A., Batalla, R. J., Vericat, D. & Balasch, J. C. Rainfall, runoff and sediment transport relations in a mesoscale mountainous catchment: The River Isábena (Ebro basin). *Catena*. **82**, 23–34 (2010).
4. Morin, E. *et al.* Spatial patterns in thunderstorm rainfall events and their coupling with watershed hydrological response. *Adv. Water Resour.* **29**, 843–860 (2006).
5. Faures, J., Goodrich, D. C., Woolhiser, D. A. & Sorooshian, S. Impact of small-scale spatial rainfall variability on runoff modeling. *J. Hydrol.* **173**, 309–326 (1995).
6. Wei, W., Chen, L. D. & Fu, B. J. Effects of rainfall change on water erosion processes in terrestrial ecosystems: A review. *Prog. Phys. Geogr.* **33**, 307–318 (2009).
7. An, J., Zheng, F. L. & Han, Y. Effects of rainstorm patterns on runoff and sediment yield processes. *Soilence*. **179**, 293–303 (2014).
8. Yan, Q. H. *et al.* Effect of rainstorm patterns and soil erosion control practices on soil and water loss in small watershed on loess plateau. *Trans. Chin. Soc. Agric. Mach.* **45**, 169–175 (2014).
9. Emmanuel, I., Andrieu, H., Leblois, E., Janey, N. & Payrastre, O. Influence of rainfall spatial variability on rainfall–runoff modeling: Benefit of a simulation approach?. *J. Hydrol.* **531**, 337–348 (2015).
10. Paschalis, A., Faticchi, S., Molnar, P., Rimkus, S. & Burlando, P. On the effects of small scale space-time variability of rainfall on basin flood response. *J. Hydrol.* **514**, 313–327 (2014).
11. Shen, Z. Y., Chen, L., Liao, Q., Liu, R. M. & Hong, Q. Impact of spatial rainfall variability on hydrology and nonpoint source pollution modeling. *J. Hydrol.* **472–473**, 205–215 (2012).
12. Zhao, F. F., Zhang, L., Chiew, F. H. S., Vaze, J. & Cheng, L. The effect of spatial rainfall variability on water balance modelling for south-eastern Australian catchments. *J. Hydrol.* **493**, 16–29 (2013).

13. Zhang, L. T., Li, Z. B., Wang, H. & Xiao, J. B. Influence of intra-event-based flood regime on sediment flow behavior from a typical agro-catchment of the Chinese Loess Plateau. *J. Hydrol.* **538**, 71–81 (2016).
14. Zhang, L. T., Gao, Z. L., Li, Z. B. & Tian, H. W. Downslope runoff and erosion response of typical engineered landform to variable inflow rate patterns from upslope. *Nat. Hazards.* **80**, 775–796 (2016).
15. Zhang, L. T., Li, Z. B. & Wang, S. S. Impact of runoff regimes on sediment yield and sediment flow behavior at slope scale. *Trans. Chin. Soc. Agric. Eng.* **619**, 754–759 (2015).
16. Wang, S. *et al.* Reduced sediment transport in the Yellow River due to anthropogenic changes. *Nat. Geosci.* **9**, 38–41 (2016).
17. Xu, G. C. *et al.* Impact of soil and water conservation on soil organic carbon content in a catchment of the middle Han River, China. *Environ. Earth Sci.* **74**, 6503–6510 (2015).
18. Boix-Fayos, C., De Vente, J., Barberá, G. G. & Castillo, V. The impact of land use change and check-dams on catchment sediment yield. *Hydrol. Process.* **22**, 4922–4935 (2010).
19. Camera, C. *et al.* Quantification of the effect of terrace maintenance on soil erosion: Two seasons of monitoring experiments in Cyprus. *Egu General Assembly Conference.* **19**, 7404 (2017).
20. Montenegro, A. A. A., Abrantes, J. R. C. B., Lima, J. L. M. P. D., Singh, V. P. & Santos, T. E. M. Impact of mulching on soil and water dynamics under intermittent simulated rainfall. *Catena.* **109**, 139–149 (2013).
21. Gao, P. *et al.* Streamflow regimes of the Yanhe River under climate and land use change, Loess Plateau, China. *Hydrol. Process.* **29**, 2402–2413 (2015).
22. Peng, T. & Wang, S. J. Effects of land use, land cover and rainfall regimes on the surface runoff and soil loss on karst slopes in southwest China. *Catena.* **90**, 53–62 (2012).
23. Mu, X. M., Zhang, L., Mcvicar, T. R., Chille, B. & Gau, P. Analysis of the impact of conservation measures on stream flow regime in catchments of the Loess Plateau, China. *Hydrol. Process.* **21**, 2124–2134 (2007).
24. Zhang, L. T., Li, Z. B. & Xiao, J. B. Effects of different flood regimes on soil erosion and sediment transport in typical small watershed of Loess Hilly Gully Region. *Trans. Chin. Soc. Agric. Mach.* **47**, 109–116 (2016).
25. Qi, J. Y. *et al.* Effects of soil and water conservation on reduction of runoff and sediment in Chabagou watershed. *Sci. Soil Water Conserv.* **8**, 28–33 (2010).
26. Xu, J. X. Erosion caused by hyperconcentrated flow on the Loess Plateau of China. *Catena.* **36**, 1–19 (1999).
27. Zheng, M. G., Li, R. K. & He, J. J. Sediment concentrations in run-off varying with spatial scale in an agricultural subwatershed of the Chinese Loess Plateau. *Hydrol. Process.* **29**, 5414–5423 (2015).
28. Li, Z. B. *et al.* Study on the soil erosion model for rainstorm based on runoff erosion power. *Proceedings of the Sixth National Symposium on the Basic Theory of Sediment.* 54–59 (2005).
29. Fang, N. F. *et al.* The effects of rainfall regimes and land use changes on runoff and soil loss in a small mountainous watershed. *Catena.* **99**, 1–8 (2012).
30. Wang, Y. X. *et al.* Effects of erosion on the microaggregate organic carbon dynamics in a small catchment of the Loess Plateau, China. *Soil Tillage Res.* **174**, 205–213 (2017).
31. Zhang, L. T. *Spatial Scale Effects on Erosive Energy Based Water Flowdriven Sediment Delivery on the Hilly Loess Region of the Chinese Loess Plateau* (The University of Chinese Academy of Sciences, 2016).
32. Hu, J. F. *et al.* Effect of soil and water conservation measures on regime-based suspended sediment load during floods. *Sustain. Cities Soc.* **55**, 102044 (2020).
33. Cui, S. Y., Song, X. Y., Li, H. Y. & Li, Y. L. The characters of different flood regimes on soil erosion and sediment transport in a typical small watershed in the gully region of the Loess Plateau. *J. Xi'an Univ. Technol.* **33**, 338–344 (2017).
34. Chang, S. G., Hu, X. Q., Shi, D. M., Ding, W. B. & Jiang, P. Characteristics of runoff and sediment, nitrogen and phosphorus loesses under soil management measures in sloping farmland. *J. Soil Water Conserv.* **30**, 34–40 (2016).
35. Chi, C. X., Hao, Z. C., Wang, L. & Hu, J. W. Study on the variation of production and confluence characteristics of Chaba gully under the influence of human activities. *The Interaction and Effect between Water and Social and Economic Development - Proceedings of the third National Symposium on Water Issues.* 119–124 (2005).
36. Chen, R. D. *et al.* Comparative analysis of flow and sediment characteristics of the Yanhe River under extreme rainfall conditions and research on influence factors. *Acta Ecol. Sin.* **38**, 1920–1929 (2018).
37. Quiñero-Rubio, J. M., Nadeu, E., Boix-Fayos, C. & Vente, J. Evaluation of the effectiveness of forest restoration and check-dams to reduce catchment sediment yield. *Land Degrad. Dev.* **27**, 1018–1031 (2016).
38. Zhao, X. N., Wu, P. T., Chen, X. L., Helmers, M. J. & Zhou, X. B. Runoff and sediment yield under simulated rainfall on hillslopes in the Loess Plateau of China. *Soil Res.* **51**, 50–58 (2013).
39. Zhang, L., Shi, C. X. & Zhang, H. Effects of check-dams on sediment storage-release in Chabagou Watershed. *Trans. Chin. Soc. Agric. Eng.* **2010**, 64–69 (2010).
40. Diyabalanage, S., Samarakoon, K. K., Adikari, S. B. & Hewawasam, T. Impact of soil and water conservation measures on soil erosion rate and sediment yields in a tropical watershed in the Central Highlands of Sri Lanka. *Appl. Geogr.* **79**, 103–114 (2017).
41. Rashid, M., Alvi, S., Kausar, R. & Akram, M. I. The effectiveness of soil and water conservation terrace structures for improvement of crops and soil productivity in rainfed terraced system. *Pak. J. Agric. Sci.* **53**, 241–248 (2016).
42. Laurencelle, J., Logan, T., Genoks, R. ASF Radiometrically Terrain Corrected ALOS PALSAR products. *ASF-Alaska Satell. Facil.* (2015).

Acknowledgements

This research was financially supported by the National Nature Science Foundation of China (41771311), the International (Regional) Cooperation and Exchange Program of the National Natural Science Foundation of China (41561144011) and the National Natural Science Foundation of China (41807066). Data support was acquired from the Loess Plateau Data Center, National Earth System Science Data Sharing Infrastructure, National Science & Technology Infrastructure of China (<http://loess.geodata.cn>). We appreciate the suggestions of the anonymous reviewer and editor.

Author contributions

S.S.W. and L.T.Z. conducted the basic data and determined the method. S.S.W. worked the data for visualization and drafted the manuscript. Z.B.L., B.M. and L.T.Z. revised the manuscript. All authors reviewed the manuscript.

Competing interests

The authors declare no competing interests.

Additional information

Correspondence and requests for materials should be addressed to Z.-B.L.

Reprints and permissions information is available at www.nature.com/reprints.

Publisher's note Springer Nature remains neutral with regard to jurisdictional claims in published maps and institutional affiliations.



Open Access This article is licensed under a Creative Commons Attribution 4.0 International License, which permits use, sharing, adaptation, distribution and reproduction in any medium or format, as long as you give appropriate credit to the original author(s) and the source, provide a link to the Creative Commons licence, and indicate if changes were made. The images or other third party material in this article are included in the article's Creative Commons licence, unless indicated otherwise in a credit line to the material. If material is not included in the article's Creative Commons licence and your intended use is not permitted by statutory regulation or exceeds the permitted use, you will need to obtain permission directly from the copyright holder. To view a copy of this licence, visit <http://creativecommons.org/licenses/by/4.0/>.

© The Author(s) 2021